Aharonov-Bohm effect in charge-density wave loops with inherent temporal current switching

M. Tsubota[1], K. Inagaki[1,2] , T. Matsuura[1] , and S. Tanda[1,2]

[1] *Department of Applied Physics, Hokkaido University, Sapporo 060-8628, Japan*
[2] *Center of Education and Research for Topological Science and Technology, Hokkaido University, Sapporo 060-8628, Japan*

PACS 71.45.Lr – Charge-density-wave systems
PACS 73.23.-b – Electronic transport in mesoscopic systems
PACS 03.65.Vf – Phases: geometric; dynamic or topological

Abstract – We report evidence for Aharonov-Bohm (AB) oscillations with temporal current switching at 5.1 and 79 K by using charge-density wave (CDW) loops in TaS_3 ring crystals. The periodicity of the AB oscillations is $h/2e$, and this is confirmed by employing four samples with different diameters. This means that sliding CDWs carry $2e$ charge quanta. We observe current switching between the two states, namely the high and low current states, as a result of the separation of field-dependent and time-dependent fluctuations. The probability distribution of the switching oscillates also with a period of $h/2e$. We discover that the observed oscillations, which are a superposition of the current fluctuations and the switching behavior, have a period $h/2e$.

Introduction. – Fifty years ago, Aharonov and Bohm challenged our understanding of vector potential, which had not been considered a physical entity [1, 2]. Since then, the concept of the AB (Aharonov and Bohm) phase has been accepted in many areas of modern physics [3] including condensed matter physics [4–8], particle physics [9], non-abelian gauge theories [10], gravitational physics [11, 12] and laser dynamics [13]. To observe the AB phase using metallic rings, the ring must be 1 μm in diameter and measured at a low temperature (typically below 1 K) to maintain quantum phase coherence [5].

The existence of the AB effect of charge-density wave (CDW) condensates has remained an open question. CDWs have not been considered to exhibit the AB effect because an electron-hole pair of a CDW has neutral charge that cannot couple to vector potential, and the CDW phase is usually treated as a classical coordinate. However, the AB effect of a CDW was first predicted by Bogachek *et al* [17]. Their model includes a term representing the interaction of the CDW with the vector potential field, and then estimates the oscillation of $h/2e$. Another theory states that quasi-particle interference is generated by changing the CDW ground state [18–20]. Latyshev *et al* tried to observe the AB effect of CDWs in $NbSe_3$ crystals with tiny random holes pierced by heavy-ion irradiation [21]. They revealed oscillation in the nonlinear CDW conductivity as a function of the magnetic field. Visscher *et al*, however, insisted that this could be the AB effect of a quasi-particle passing through a metallic region, where the CDW order was destroyed near the tiny holes [22]. For this reason, a CDW loop, over which the continuity of the CDW order is maintained, should be employed to settle the argument.

Topological crystals (ring and Möbius strip shaped seamless crystals) [14, 23] are the only materials providing such a CDW loop. The chain axis of a CDW directs itself along the circumference of the ring without losing the CDW order, thereby forming a CDW loop. This cannot be realized simply by piercing a hole in a conventional single crystal, because a continuous CDW chain is not formed by the hole.

We report the first evidence for the AB interference effect with temporal current switching at a high temperature of 79 K by using CDW loops in TaS_3 ring crystals whose circumferences are as long as 85 μm. We investigated orthorhombic TaS_3, which has a Peierls transition at 218 K, and no uncondensed electrons at low temperatures. Current switching between two states, namely high

and low current states, occurs in a time-dependent fluctuation. The CDW condensate maintained macroscopic phase coherence, which extended over the ring system [15]. The periodicity of the AB effect of the CDW was half a flux quantum $h/2e$ with h and e being Planck's constant and the elementary charge, respectively.

Experiments and results. – The samples were synthesized by the chemical vapor transport method [14]. The materials (tantalum and sulfur) were reacted in an evacuated quartz tube to produce TaS_3 crystals (whisker, ring and other kinds of topological crystals). We prepared a ring/tube crystal reproducibly (fig. 1(a)), and then cut one with a focused ion beam (fig. 1(c)). We fabricated gold electrodes on the sample using electron-beam lithography [24], after coating it with polymethylmethacrylate (fig. 1(b)). We measured the temperature dependence of the resistivity to identify the ring crystal. As a result, the properties of our sample agreed with the previously reported properties of a conventional whisker of orthorhombic TaS_3 [16].

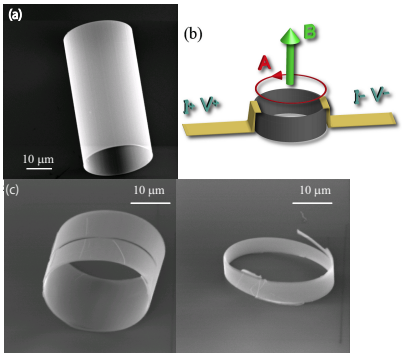

Fig. 1: (a) Scanning electron microscope (SEM) image of a TaS_3 tube-shaped crystal. (b) Contact configuration for transport measurement. Two gold electrodes (100 nm thick, 5 μm wide) were evaporated. (c) SEM image of a TaS_3 tube/ring crystal (left) before cutting, (right) after cutting.

We measured the dc electric current at 5.1 K while applying a magnetic field in the vertical direction to the ring crystal, which was 27 μm in diameter and 1×0.1 μm^2 in cross-sectional area. The magnetic field was swept at a sweep rate of 50 μGauss/sec which is slow enough to prevent the generation of eddy current. Each data set consisted of an average of 10 raw current values measured every five seconds with a time constant of 100 ms. The magnetoresistance of a TaS_3 ring crystal is shown at voltages of 100, 200 and 300 mV, in fig. 2(a). We observed periodic oscillations in these voltages that increased in amplitude when we increased the voltage.

We calculated the power spectra of the observed oscillations using the discrete Fourier transform (DFT) and the maximum entropy method (MEM) for an accurate structural analysis. In particular, MEM analysis can detect the

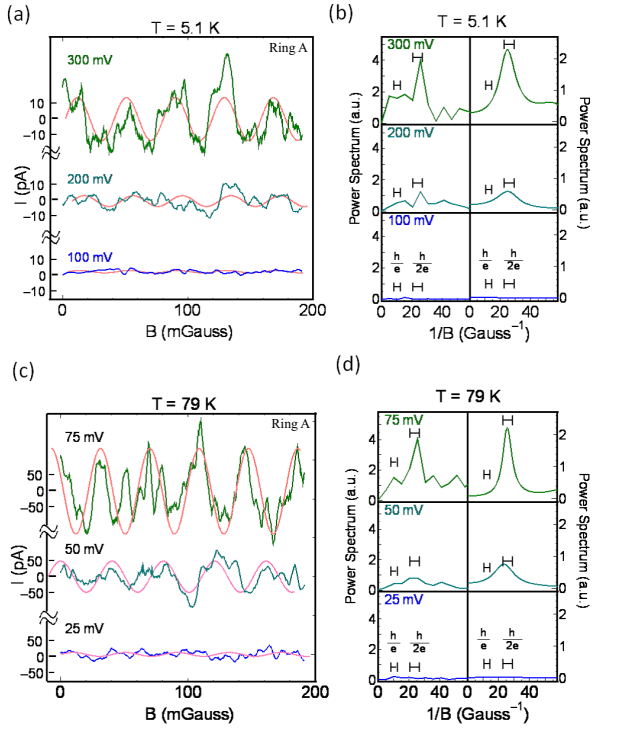

Fig. 2: (a) Change in current value as magnetic field at 5.1 K, applied voltage 100, 200 and 300 mV. (b) The power spectra of the observed oscillation using DFT (left) and MEM (right). The red lines show the sinusoidal oscillation estimated by IDFT and MEM. (c) Current depending on magnetic field and (d) the evolution of the power spectra DFT (left) and MEM (right), 25, 50 and 75 mV, from bottom to top at 79 K.

peaks of a signal that includes noise. Fig. 2(b) shows the evolution of the power spectra using DFT (left) and MEM (right), 100, 200 and 300 mV, from bottom to top. The oscillation period ΔB estimated from the power spectra is 40 mGauss for all voltages. By assuming that the origin of the oscillation is the AB effect, we estimated the effective charge e^* using the following formula,

$$\Delta B = \frac{\Phi_0}{S} = \frac{h}{e^*} \cdot \frac{1}{\pi r^2} \tag{1}$$

where h is Planck's constant and r is the radius of the ring crystal. The estimated value of an effective charge e^* is 3.0×10^{-19} C, and this is approximately equal to two times the elementary charge ($2e = 3.2 \times 10^{-19}$ C).

We confirmed the period $h/2e$ of the main peak by the following analyses. The position of the main peak was determined with MEM, and then the amplitude and the phase of the corresponding peak were obtained from the DFT. This was why many peaks were observed caused by narrow band noise or extrinsic noise using DFT, and why the main peak was blurred. Using MEM, we carefully analyzed the magnetoresistance oscillation compared with DFT for the disappearance of false peaks [25]. The red lines in fig. 2(a) show the sinusoidal oscillation with the

period estimated by MEM and the amplitude estimated by the inverse DFT (IDFT) of the main peak. The major contribution of the observed oscillations is well expressed by the obtained spectra. Other peaks, such as h/e or $h/4e$, were not observed.

The oscillation period with data at 79 K agreed with that at 5.1 K (fig. 2(c)). Fig. 2(d) shows the evolution of the power spectra, 25, 50 and 75 mV, from bottom to top. The estimated value of an effective charge e^* is 3.1×10^{-19} C, which the corresponds to the value at 5.1 K. The periodic oscillation $h/2e$ remained in magnetoresistance at 79 K. It is noteworthy that at such a high temperature usually thermal fluctuation destroys quantum coherence.

In addition, four samples with different diameters showed the periodic oscillation $h/2e$. We measured the magnetoresistance of the ring crystals, whose diameters were 4.9, 12 and 17 μm, respectively. The observed periods were 1.3, 1.8×10^{-1} and 9.9×10^{-2} Gauss, which were 1.2, 1.1 and 1.1 in $h/2e$ units, respectively. Four samples showed a periodicity of $h/2e$. The periodic oscillation depended only on the magnetic flux penetrating the ring. Our previous report [26] showed the voltage-current characteristics of the Ring A sample. In fact, the CDW current and the amplitude of the oscillation behaved similarly, in particular, there was a significant increase in V_T. All four samples behaved in the same way. The increase in the amplitude with respect to $h/2e$ oscillation can be plausibly attributed the development of a sliding CDW. These results are summarized in Table 1.

To consider the observed current fluctuations without the period, it is necessary to rule out the possibility of an experimental artifact. The resistance may vary significantly with a tiny change of temperature because the temperature dependence of the sample obeys the Arrhenius-type activation. In our experiment, the temperature varied no more than 10^{-3} K, so the current fluctuation was not caused by a temperature change. In addition, the narrow band noise (NBN) in sliding CDWs should be considered. Our experimental circuit includes low-pass filters with a time constant of 10^{-3} s, as well as the numerical averaging of obtained signals. Hence the measurement is insensitive to NBN signals, typically, fluctuations with a 10^{-6} s period. Thus the $h/2e$ periodic oscillation is inherent in the sample, and should not to be attributed to experimental noises or to thermal fluctuations.

We note that the magnetoresistance seems to include some unspecified components rather than the sinusoidal oscillation corresponding to the peak in the power spectrum, as shown in fig. 2 (c). The conventional field sweep measurement may have been smeared by time-domain fluctuations with a long time constant. Hence we separated the field-dependent fluctuations from the time-dependent fluctuations by using the following procedure.

1. 500 current data, $I(B_0, 1)$, $I(B_0, 2)$, $I(B_0, 3)$, $\cdots$, and $I(B_0, 500)$, were measured once per second with a time constant of 200 ms in a fixed magnetic field B_0.
2. Next, 500 current data, $I(B_1, 1)$, $I(B_1, 2)$, $I(B_1, 3)$, $\cdots$, and $I(B_1, 500)$, were obtained at $B_1 = B_0 + \delta B$, which corresponded to $\sim 1/10$ step of a flux quantum, $h/2e$, as shown in fig. 3(a).
3. Consequently, time-domain current data $I(B_i, k)$ at $B_2 = B_1 + \delta B$, $B_3 = B_2 + \delta B$, $\cdots$, and $B_{49} = B_{48} + \delta B$ were obtained (fig. 3(b)).
4. The time-averaged current value was calculated by $I(B_i) = \sum_k I(B_i, k)/500$ for each fixed field B_i (shown with red squares in fig. 3(b), (c) and (d)). By employing this averaging, time-domain fluctuations were canceled if their time constants were faster than 500 seconds. Since the averaging is performed only in the time domain, we can separate field-domain fluctuations from time-domain fluctuations.
5. Finally, DFT was performed on the time-averaged data $I(B_i)$ (fig. 3(d)) to extract periodic components that depend only on magnetic field (fig. 3(e)).

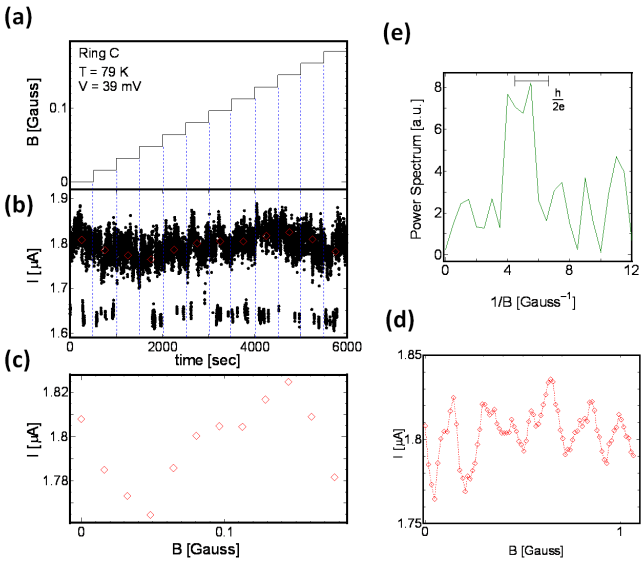

Fig. 3: Measurements and analysis technique. Time-dependence of (a) magnetic field and (b) the electric current. (c) Relation between the current and magnetic field. (d) Current data applied with high magnetic field. (e) DFT performed on the time-averaged data $I(B_i)$ to extract periodic components which depend only on magnetic field.

This procedure revealed the existence of current fluctuations in both the time and field domains (fig. 3(b)). The measurement current switched between two states, namely a high current state and a low current state. The switching occurred at intervals of a few seconds to several hundred seconds. The current of the ring had a bimodal distribution. Our discovery of temporal switching phenomena is crucial in terms of verifying the observed oscillations in a CDW.

Table 1: List of the periodic oscillation of four samples at 5.1 and 79 K. D is the diameter of the ring crystals, ΔB is the period in the oscillation of magnetoresistance, Φ is ΔB multiplied by the area of the ring crystal, Φ_0 is $h/2e$ and i_{pp} are the amplitudes of the periodic oscillation resulting from each voltage.

T = 79 K	D (μm)	ΔB (Gauss)	Φ/Φ_0	V_T (mV)	i_{pp} [V_T] (A)	i_{pp} [3V_T] (A)	i_{pp} [5V_T] (A)
Ring A	27	4.1×10^{-2}	1.1	25	3.9×10^{-11}	2.8×10^{-10}	7.0×10^{-10}
Ring B	17	9.9×10^{-2}	1.1	50	6.0×10^{-11}	3.0×10^{-10}	9.1×10^{-10}
Ring C	12	1.8×10^{-1}	1.0	24	7.0×10^{-8}	3.0×10^{-7}	1.1×10^{-6}
Ring D	4.9	1.3	1.2	32	5.0×10^{-10}	2.1×10^{-9}	—
T = 5.1 K	D (μm)	ΔB (Gauss)	Φ/Φ_0	V_T (mV)	i_{pp} [V_T] (A)	i_{pp} [3V_T] (A)	i_{pp} [5V_T] (A)
Ring A	27	4.0×10^{-2}	1.1	110	3.6×10^{-13}	2.6×10^{-11}	8.0×10^{-11}
Ring B	17	9.5×10^{-2}	1.0	250	1.5×10^{-11}	6.5×10^{-11}	2.0×10^{-10}
Ring C	12	—	—	—	—	—	—
Ring D	4.9	1.3	1.2	190	5.1×10^{-12}	3.0×10^{-11}	3.9×10^{-10}

Since the switching interval was shorter than the averaging time (500 seconds), the averaged current was expected to exclude time-domain fluctuations, as shown in fig. 3(c). Fig. 3(d) shows the relationship between the current and the high magnetic field. This confirms unambiguously the existence of magneto-oscillations. The DFT of the oscillations is also shown in fig. 3(e). The oscillation period was $h/2e$, which is consistent with the results in fig. 2, and our previous report [26].

We investigated the switching phenomenon in detail. Fig. 4(a) shows the time dependence of the electric current when constant voltages are applied for 3000 seconds at 79 K. As a result, we observed two values of the current in a ring crystal. The panels in the figure show the applied magnetic field $\Phi/\Phi_0 = 0, -1/4, -1/2, -3/4 and -1$ from top to bottom (Φ_0 is $h/2e$). The distribution of the two states changed according to the applied field. Fig. 4(c) shows the peak currents of the two states as a function of the magnetic field. The peak current of the high current state oscillated significantly, whereas that of the low current state remained almost constant. Fig. 4(d) shows the product of the full width at half maximum (FWHM) and the peak height P, which correspond to the probability of the states. The probability of the high current state oscillated in a similar manner to the peak current. The oscillation period was 170 ± 10 mGauss. Surprisingly, this period corresponds to the flux quantum $h/2e$. Conformity between the peak current and the probability of the high current state mean that the periodic oscillation shown in fig. 2 was a superposition of the current fluctuations and the switching behavior.

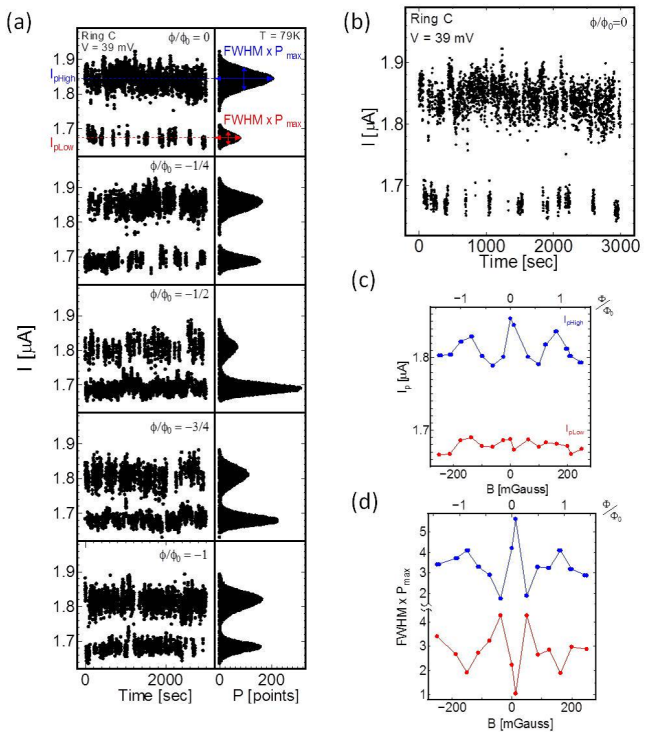

Fig. 4: (a) Time dependence of the electric current for applying constant voltages for 3000 seconds at 79 K. (b) Top panel zoomed in. (c) Peak currents of the two states as a function of the magnetic field. (d) The product of the full width at half maximum (FWHM) and the peak height P_{max}, which are corresponding to the areas of the states.

Discussion. – In our results, we discovered three phenomena in the ring crystal, namely, the periodic oscillation of the CDW current, the switching behavior, and the oscillation of the distribution of the two states of the electric current. The period was $h/2e$ corresponding to the area of the ring crystals. We discuss these phenomena, which were not observed in the whisker crystal, below.

The periodic oscillations are unlikely to originate from normal carriers generated by the conversion process. When a normal current is converted into a CDW, a CDW phase-slip is induced [27]. The CDW strain energy $F \propto (\partial\theta/\partial x)^2$ near the electrode is larger than that at the center. Hence, the energy is increased near the electrodes and a phase-slip is induced near the electrodes. Therefore, regardless of the size, the conversion process

only takes place near the electrodes [28,29]. This scenario is valid unless the spacing between the electrodes is too small, namely a few micrometers [30]. With our sample, which was 85 μm in circumference, the region is estimated to be several micrometers from the electrodes. In this context, the carriers generated by the process do not exist over the ring crystal. Next, we discuss the carrier lifetime τ to determine whether the carrier travel over the ring crystal. τ is represented by $k_BT = h/\tau \sim \Delta E$ since the quantum state of the carrier is blurred with the thermal fluctuation k_BT, where k_B is the Boltzmann constant, T is temperature and h is Planck's constant, respectively. The traveling length l of the carrier in the system is estimated as $l = v_F\tau$, where v_F is the Fermi velocity estimated as 10^6 m/s. l is calculated to be 10 μm at 5.1 K and about 600 nm at 79 K. Since the circumference is 85 μm, the carrier will not travel and its phase is unlikely to be preserved over the whole system at 79 K. With our sample, the possibility of the Al'tshuler-Aronov-Spivak (AAS) effect [6], namely the $h/2e$ oscillation of a quasi-particle, is ruled out.

With a sliding CDW, AB interference occur in our sample length because the correlation length is long. This length was reported to be longer than 100 μm from an estimation of the size effect in the sliding CDW [31, 32]. Another estimation provided a value of about 1 μm by using the X-ray scattering technique [33,34]. The reason for the difference between these lengths remains unclear. We consider that the phase correlation length in our samples reaches about 100 μm from the circumference. The $NbSe_3$ ring crystals also have a correlation length of about 100 μm as determined by Shapiro step experiment [35]. These results are consistent with length results reported in the sliding state [31, 32].

Our study shows that the periodicity of CDW interference is half a flux quantum $h/2e$, which is the same as for a superconductor resulting from Cooper pairing. Bogachek *et al* [17] suggested that the charge quanta of CDWs are multiples of the chain number. For example, the interference of a single CDW chain results in the period $h/2e$, while a bundle of CDWs with N chains provides an oscillation with a period of $h/2Ne$. If a transverse correlation between CDWs forms CDW bundles, a period of $h/4e$ or $h/8e$ must be observed. In fact, the power spectra only gives the fundamental $h/2e$ oscillation. Thus we proposed a model to describe the $h/2e$ oscillation in our previous report [26]. This model showed a CDW soliton confined in a single chain encircled by a dislocation loop, carrying a charge of $2e$ per chain [37, 41, 42]. The existence of the dislocation loop makes the soliton move freely along the chain accompanying the $2e$ charge. Then the charge neutrality is preserved by the creation of soliton-antisoliton pairs. The AB amplitude represents the total of these confined chains and about 8 % of all CDW chains. In the context, the soliton excitation is the origin of the $2e$ charge in a CDW.

Now we consider the two states indicated by the switching of the electric current. Assume that a soliton pair is created when the CDW slides [36,37]. When a soliton pair is created, a voltage ΔV is generated between the solitons. Thus the soliton pair is accompanied by a voltage different from the initial voltage due to the relaxation of CDW strain, which may drive a circulating current in the CDW loop [35]. Fig. 5(a) and (b) are schematics showing cases where a soliton pair was absent and present, respectively. The ammeter measures the sum of the currents that flow in the left and the right arms, namely, $I = I_1 + I_2$, $(I_1 = V_0/R_R, I_2 = V_0/R_L)$, where R_R and R_L are the resistances of the right and left arms, respectively. It should be noted that the ammeter does not measure the circulating current through path 3. The sign of ΔV is opposite to that of the applied voltage V_0, because the soliton pair generation relaxes the strain energy of the CDW. Within this closed circuit, according to the Kirchhoff's law,

$$I_1R_R = V_0 - \Delta V, \tag{2}$$

$$I_2R_L = V_0, \tag{3}$$

$$-I_1R_R + I_2R_L = \Delta V. \tag{4}$$

As a result, I_1 and I_2 are equal to $(V_0 - \Delta V)/R_R$ and V_0/R_L. Consequently, the total current for the latter case is $\Delta V/R_R$ smaller than that of the former case. Hence the current can be either of the two values representing the switching between the two states, namely the value shows whether or not the phase slip has occured.

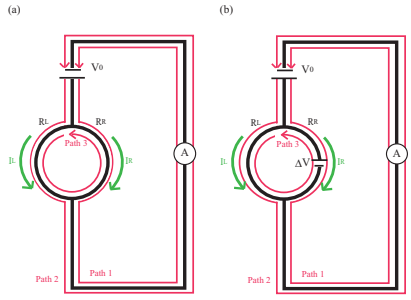

Fig. 5: Schematic picture of two current states. (a) absent and (b) present of the voltage ΔV generated by soliton pair.

Next, we consider the point distribution of two states. The probability of high current state behaves similarly to the current peak as a function of a magnetic field. When we consider whether or not a phase slip occurs, the probability distribution of the soliton-antisoliton pair created by the phase slip appears to oscillate depending on the field. The period can be realized as it fits the AB phase. The switching interval of the order of several seconds is not explained by the NBN or other CDW phenomena in the whisker [38, 39]. The enhancement of the periodic boundary condition originating from the ring topology may play an important role in relation to the CDW phase [35, 40]. The distribution change is obviously related to the CDW

loop, and the resolution of the dynamics requires further experiments.

Our result implies that a persistent CDW current should be present since the electric charge in a sliding CDW is coupled with the vector potential. Our group has already synthesized NbS_3 ring crystals [43] in which a Peierls transition occurs at room temperature. In the context, it will be necessary to reconsider the possibility of Fröhlich-type superconductivity [44, 45] and a room temperature operating quantum interference device.

* * *

The authors are grateful to T. Toshima, T. Tsuneta, K. Matsuda, K. Ichimura, and K. Yamaya, for experimental support and Y. Asano, M. Hayashi, N. Hatakenaka, and P. Monceau for stimulating discussions. This research has been supported by Grant-in-Aid for the 21st Century COE program on " Topological Science and Technology " and the Japan Society for the Promotion of Science.

REFERENCES

[1] Y. Aharonov and D. Bohm, Phys. Rev. **115** (1959) 485.
[2] W. Ehrenberg and R. E. Siday, Proc. Phys. Soc. **B62** (1949) 8.
[3] A. Tonomura, T. Matsuda, R. Suzuki, A. Fukuhara, N. Osakabe, H. Umezaki, J. Endo, K. Shinagawa, Y. Sugita, and H. Fujiwara, Phys. Rev. Lett. **48** (1982) 1443.
[4] W. A. Little and R. D. Parks, Phys. Rev. Lett. **9** (1962) 9.
[5] R. A. Webb, S. Washburn, C. P. Umbach and R. B. Laibowitz, Phys. Rev. Lett. **54** (1985) 2696.
[6] B. L. Al'tshuler, A. G. Aronov and B. Z. Spivak, JETP Lett. **33** (1981) 94.
[7] Y. Aharonov and A. Casher, Phys. Rev. Lett. **53** (1984) 319.
[8] M. König, A. Tschetschetkin, E. M. Hankiewicz, J. Sinova, V. Hock, V. Daumer, M. Schäfer, C. R. Becker, H. Buhmann, and L. W. Molenkamp, Phys. Rev. Lett. **96** (2006) 076804.
[9] T. T. Wu and C. N. Yang, Phys. Rev. D **12** (1975) 3845.
[10] P. A. Horváthy, Phys. Rev. D **33** (1986) 407.
[11] L. H. Ford and A. Vilenkin, J. Phys. A: Math. Gen. **14** (1981) 2353.
[12] A. Ashtekar and A. Magnon, J. Math. Phys. **16** (1975) 341.
[13] O. Hosten and P. Kwiat, Science **319** (2008) 787.
[14] S. Tanda, T. Tsuneta, Y. Okajima, K. Inagaki, K. Yamaya, and N. Hatakenaka, Nature **417** (2002) 397.
[15] G. Grüner, *Density Waves in Solids* (Addison-Wesley, Reading, MA, 1994), and references therein.
[16] T. Sambongi, K. Tsutsumi, Y. Shiozaki, M. Yamamoto, K. Yamaya, and Y. Abe, Solid State Comm. **22** (1977) 729.
[17] E. N. Bogachek, I. V. Krive, I. O. Kulik, and A. S. Rozhavsky, Phys. Rev. B **42** (1990) 7614.
[18] M. I. Visscher, B. Rejaei, and G. E. W. Bauer, Euro. Lett. **36** (1996) 613.
[19] J. Yi, M. Y. Choi, K. Park, and E.-H Lee, Phys. Rev. Lett. **78** (1997) 3523.
[20] G. Montambaux, Euro. Phys. Jour. **1** (1998) B377.
[21] Yu. I. Latyshev, O. Laborde, P. Monceau, and S. K. Klaumunzer, Phys. Rev. Lett. **78** (1997) 919.
[22] M. I. Visscher and B. Rejaei, Euro. Phys. Lett. **43** (1998) 617.
[23] T. Matsuura, M. Yamanaka, N. Hatakenaka, T. Matsuyama, and S. Tanda, J. Crys. Grow. **297** (2006) 157.
[24] K. Inagaki, T. Toshima, S. Tanda, K. Yamaya and S. Uji, Appl. Phys. Lett. **86** (2005) 073101.
[25] Since MEM algorithm may suggest spurious or wide peaks if an inappropriate parameter is used, we carefully chose MEM parameter for the spectral line width of MEM being as wide as that of DFT. MEM and DFT were conducted with the following bibliography, W. H. Press *et al*, *NUMERICAL RECIPES, Third edition* (Cambridge University Press, New York, 2007).
[26] M. Tsubota, K. Inagaki, and S. Tanda, Physica B **404** (2009) 416.
[27] S. Ramakrishna, M. P. Maher, V. Ambegaokar and U. Eckern, Phys. Rev. Lett. **68** (1992) 2066.
[28] T. L. Adelman, M. C. de Lind van Wijngaarden, S. V. Zaitsev-Zotov, D. DiCarlo and R. E. Thorne, Phys. Rev. B **53** (1996) 1833.
[29] S. G. Lemay, M. C. de Lind van Wijngaarden, T. L. Adelman and R. E. Thorne, Phys. Rev. B **57** (1998) 12781.
[30] O. C. Mantel, F. Chalin, C. Dekker, H. S. J. van der Zant, Yu. I. Latyshev, B. Pannetier and P. Monceau, Phys. Rev. Lett. **84** (2000) 538.
[31] J. W. Lyding, J. S. Hubacek, G. Gammie and R. E. Thorne, Phys. Rev. B **33** (1986) 4341.
[32] G. Mihály, Gy. Hutiray and L. Mihály, Phys. Rev. B **28** (1983) 4896.
[33] K. L. Ringland, A. C. Finnefrock, Y. Li, J. D. Brock, S. G. Lemay, and R. E. Thorne, Phys. Rev. B **61** (2000) 4405.
[34] R. Danneau, A. Ayari, D. Rideau, H. Requardt, J. E. Lorenzo, L. Ortega, P. Monceau, R. Currat and G. Grübel, Phys. Rev. Lett. **89** (2002) 106404-1.
[35] T. Matsuura, K. Inagaki and S. Tanda, Phys. Rev. B **79** (2009) 014304-1.
[36] J. H. Miller, Jr, G. Cárdenas, A. Gercía-Perez, W. More and A. W. Beckwith, J. Phys. A: Math. Gen. **36** (2003) 9209.
[37] K. Maki, Phys. Rev. Lett. **39** (1977) 46.
[38] N. P. Ong, G. Verma and K. Maki, Phys. Rev. Lett. **52** (1984) 663.
[39] N. P. Ong, C. B. Kalem and J. C. Eckert, Phys. Rev. B **30** (1984) 2902.
[40] K. Shimatake, Y. Toda and S. Tanda, Phys. Rev. B **73** (2006) 153403.
[41] J.-M. Duan, Phys. Rev. B **48** (1993) 4860.
[42] N. Hatakenaka, M. Shiobara, K. Matsuda and S. Tanda, Phys. Rev. B **57** (1998) R2003.
[43] T. Tsuneta: private communication.
[44] H. Fröhlich, Proc. R. Soc. London Ser. A **223** (1954) 296.
[45] M. J. Rice, A. R. Bishop, J. A. Krumhansl and S. E. Trullinger, Phys. Rev. Lett. **36** (1976) 432.